ACS Catalysis

pubs.acs.org/acscatalysis Letter

Resolving the Types and Origin of Active Oxygen Species Present in Supported Mn-Na_2WO_4/SiO_2 Catalysts for Oxidative Coupling of Methane

Sagar Sourav, Yixiao Wang,* Daniyal Kiani, Jonas Baltrusaitis,* Rebecca R. Fushimi,* and Israel E. Wachs*

Cite This: *ACS Catal.* 2021, 11, 10288–10293 Read Online

ACCESS | Metrics & More | Article Recommendations | Supporting Information

ABSTRACT: The involvement of lattice oxygen species is important toward oxidative coupling of the methane reaction (OCM) over supported Mn-Na_2WO_4/SiO_2 catalysts, but there is no consensus regarding the types, role, and origin of lattice oxygen species present in supported Mn-Na_2WO_4/SiO_2 catalysts, which hinders the understanding of the OCM reaction network. In the present study, by utilizing the temporal analysis of products technique, we show that supported Na_2WO_4/SiO_2 catalysts possess two different types of oxygen species, dissolved O_2 and atomic O, at an OCM-relevant temperature. The addition of Mn-oxide to this catalyst increases the total amount and release rate of dissolved O_2 species and improves C_2 selectivity of both dissolved O_2 and atomic lattice O species.

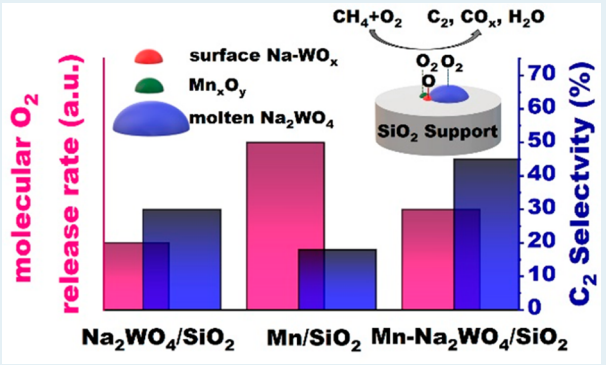

KEYWORDS: *Mn-Na_2WO_4/SiO_2 catalyst, oxidative coupling of methane (OCM), lattice oxygen, dissolved oxygen, molten salt, temporal analysis of products (TAP)*

Oxidative coupling of methane (OCM) offers great potential for the single-step conversion of natural gas to value-added C_2 products.[1] Among hundreds of catalysts tested for the OCM reaction, the supported Mn-Na_2WO_4/SiO_2 catalyst exhibits excellent thermal stability and high C_2 product yield.[2,3] The obtained C_2 yield, however, needs further improvement for achieving practical industrial application. This demands an advanced molecular-level understanding of the Mn-Na_2WO_4/SiO_2 catalysts' structure and the associated OCM reaction mechanism.[3]

The complexity of the OCM reaction mechanism arises from the involvement of both gas-phase and surface reaction networks. Additionally, multiple types of lattice oxygen species in Mn-Na_2WO_4/SiO_2 catalysts have been proposed to contribute toward the OCM reaction in a Mars–van Krevelen type mechanism that further complicates the catalytic system.[4−7] A summary of the types of lattice oxygen species is given in Table 1 and briefly discussed below.

The conversion of CH_4 over Mn-Na_2WO_4/SiO_2 catalysts, in the absence of gas-phase molecular O_2, indicates the involvement of lattice oxygen species.[5,8] Additionally, pulses of CH_4+$^{18}O_2$ gas mixtures over Mn-Na_2WO_4/SiO_2 catalysts (preoxidized with $^{16}O_2$) produced both ^{16}O- and ^{18}O-containing CO_x products.[9] This further highlights the importance of lattice oxygen toward the OCM reaction mechanism. The first detailed investigation of the nature of lattice oxygen species was conducted by sequential pulsing of O_2-CH_4 in a temporal analysis of products (TAP) reactor, with only C_2H_6 and CO_2 as OCM products.[4] The amount of CO_2 produced decreased with increasing time spacing between O_2 and CH_4 pulses, while the C_2H_6 formation amount remained unaltered. This is possible if at least two different types of lattice oxygen species, loosely bound and strongly bound, are involved in the formation of CO_2 and C_2H_6 products, respectively.[4] A subsequent study utilizing anaerobic CH_4, C_2H_6, and C_2H_4 temperature-programmed reduction (TPR) experiments proposed that electrophilic and nucleophilic lattice O species are responsible for C_2 and CO_x product formation, respectively.[5] In a different investigation, the activation energy values for C_2 and CO formation were found much higher than that of CO_2 formation.[9] This suggests CO_2 formation must come from one type of site containing a loosely bound oxygen species, whereas the CO and C_2 products form on a second type of site possessing a strongly

Received: May 23, 2021
Revised: July 19, 2021
Published: August 3, 2021

https://doi.org/10.1021/acscatal.1c02315
ACS Catal. 2021, 11, 10288–10293

Table 1. Types, Role, and Origin of Lattice Oxygen Species Proposed in the Literature of Supported Mn-Na_2WO_4/SiO_2 Catalysts for the OCM Reaction

refs	approach	lattice oxygen types	lattice oxygen role	associated oxide phase
4	temporal analysis of products (TAP)	loosely bound	CO_2 formation	not reported
		strongly bound	C_2H_6 formation	
5	anaerobic CH_4, C_2H_6 and C_2H_4 temperature- programmed reduction	strongly bound:		not reported
		O* electrophilic	C_2 formation	
		O* nucleophilic	CO_x formation	
9	activation energy calculated from steady-state OCM	loosely bound	CO_2 formation	not reported
		strongly bound	CO and C_2 formation	
6	temperature-programmed (O_2) desorption and (CH_4) reduction	weakly bound	only weakly bound oxygen species were proposed responsible for OCM reaction	molten Na_2WO_4
		strongly bound		not assigned
7	enthalpy calculation by calorimetric study	weakly bonded		Mn-oxide phases
		strongly bonded		W-oxide phases
10	in situ and operando Raman, XRD; thermogravimetric analysis with MS	O_2* species, reversibly exchanging between catalyst lattice and gas phase	responsible for OCM	Na_2O inside molten Na_2WO_4; the redox cycle of Mn_7SiO_{12} and $MnWO_4$ phases expedites the O_2* release from molten Na_2WO_4

bound oxygen species. However, none of the above investigations reports the origin of lattice oxygen species observed in the corresponding studies.

Attempts to determine and assign the source of the lattice oxygen species present in the supported Mn-Na_2WO_4/SiO_2 catalysts are limited. One investigation reported the presence of two different types of lattice oxygen species, strongly bound and weakly bound, which can be removed from the catalyst by CH_4 or H_2 reduction above 600 °C and by temperature-programmed desorption above 650 °C, respectively.[6] This study speculated the transition of Na_2WO_4 from crystalline to molten phase as the reason behind the release of weakly bound oxygen species. In contrast, a follow-up study utilizing calorimetric measurements of the enthalpy change for multiple reduction and oxidation steps of Mn- and W-oxide phases suggested the weakly bound oxygen is associated with the Mn-oxide phase, while strongly bound oxygen originates from the reduction of W-oxide phases.[7] However, in situ Raman, X-ray diffraction (XRD), and thermogravimetric analysis pointed out that the sodium oxide (Na_2O) present in the Na_2WO_4 molten phase is responsible for the reversible exchange of oxygen (O_2) between the catalyst lattice and gas phase, and the redox cycle of Mn-oxide phases in $Mn^{2+}WO_4$ and $Mn^{2+}Mn^{3+}{}_6SiO_{12}$ further expedite this process.[10] However, the same study did not provide experimental evidence for the presence of Na_2O species.[10] Moreover, the Mn_7SiO_{12} and $MnWO_4$ phases, proposed to be crucial for lattice oxygen release and storage, are not observed with other in situ investigations under OCM reaction conditions.[11−15] These observations suggest that the catalytic OCM reaction can proceed even in the absence of these oxide phases (Na_2O, Mn_7SiO_{12}, $MnWO_4$) and raise questions regarding the role of these 3D phases toward the lattice oxygen exchange.

A complete fundamental understanding of the types and nature of lattice oxygen species is important for correctly establishing the OCM reaction mechanism for the supported Mn-Na_2WO_4/SiO_2 catalyst. Moreover, knowledge about the structure of the working catalyst will assist in rational catalyst development by identifying the source oxide phases of these lattice oxygen species. Recent in situ Raman and XRD studies show that the crystalline Na_2WO_4 phase melts in the high-temperature OCM reaction environment.[10−15] The crystalline Mn_2O_3 phase also becomes unstable and reduces during OCM.[12,14,15] Surface Na-WO_x sites are also present and are thermally stable and catalytically active for the OCM reaction.[16,17] These recent structural insights warrant advanced investigation of the lattice oxygen species of Mn-Na_2WO_4/SiO_2 catalyst, which is the focus of the current study.

The unique TAP features (controlled pulse size with excellent time resolution for probing the catalytic sites in a time-resolved manner)[18] are applied in the present investigation to address the (*i*) types of oxygen species present in supported Na_2WO_4/SiO_2 catalysts at OCM reaction temperatures, (*ii*) origin and nature of these oxygen species with regards to the oxide phases present in Na_2WO_4/SiO_2 catalysts, and (*iii*) effect of Mn toward the formation of oxygen species in the conventional Mn-Na_2WO_4/SiO_2 OCM catalysts. The details of the catalyst synthesis, structure, and experimental protocols are provided in the Supporting Information.

$^{16}O_2$-$^{18}O_2$ PUMP−PROBE EXPERIMENTS

In the $^{16}O_2$-$^{18}O_2$ pump−probe experiment, oxygen activation by the catalytic active phases was studied by introducing a

https://doi.org/10.1021/acscatal.1c02315
ACS Catal. 2021, 11, 10288−10293

pulse of $^{16}O_2$ (pump pulse) into the catalyst bed, followed by an $^{18}O_2$ pulse (probe pulse), with a fixed time delay between these pulses. For the $5Na_2WO_4/SiO_2$ catalyst at 800 °C (see Figure 1), desorption of molecular $^{16}O_2$ is observed coincident

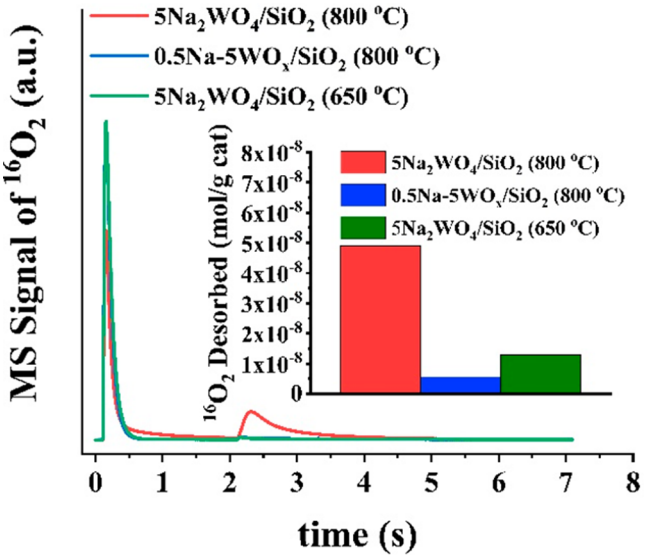

Figure 1. Mass-spectrometer (MS) response of $^{16}O_2$ during $^{16}O_2$-$^{18}O_2$ pump−probe experiment (pump−probe spacing, Δt = 2 s). The inset shows the quantified $^{16}O_2$ evolution, coincident with the injection of $^{18}O_2$ pulse.

to the secondary $^{18}O_2$ probe pulse. The $5Na_2WO_4/SiO_2$ catalyst contains both surface Na-WO_x sites and molten Na_2WO_4 phase at 800 °C (see Figure S 1 and associated discussion). To better understand the origin of this molecular $^{16}O_2$ species, the same experiment was repeated for 0.5Na-$5WO_x/SiO_2$ catalyst (at 800 °C), which possesses only the surface Na-WO_x sites (see Figure S 1). Interestingly, desorption of $^{16}O_2$ was not observed from the surface Na-WO_x phase, confirming that Na_2WO_4 is the source oxide phase for $^{16}O_2$ species. Further, when the temperature of the $5Na_2WO_4/SiO_2$ catalyst was decreased to 650 °C, below the melting temperature (~698 °C) of crystalline Na_2WO_4, the pulse response of $^{16}O_2$, coincident with secondary $^{18}O_2$ pulse, drastically decreased, indicating that only molten Na_2WO_4 phase is capable of releasing $^{16}O_2$ species. Additional investigation and analysis of $^{16}O_2$ evolution from these two catalysts at different temperatures (see Figure S 2 and associated discussion) suggested that the $^{16}O_2$ species released by $5Na_2WO_4/SiO_2$ catalysts are due to the desorption of dissolved oxygen from the molten Na_2WO_4 phase.

■ ANAEROBIC $^{13}CH_4$ SERIES PULSING

To identify other possible kind of oxygen species, an anaerobic OCM reaction was conducted over the $5Na_2WO_4/SiO_2$ catalyst at 800 °C by pulsing only $^{13}CH_4$/Ar. During the initial pulses of $^{13}CH_4$ (see Figure 2), molecular O_2 desorption from the $5Na_2WO_4/SiO_2$ catalyst was observed. No such desorption of dissolved molecular oxygen species was observed when the same experiment was conducted over the 0.5Na-$5WO_x/SiO_2$ catalyst at 800 °C (see Figure S 4). This further verifies that the $^{16}O_2$ response from $5Na_2WO_4/SiO_2$ catalyst comes from the molten Na_2WO_4 phase. Interestingly, even after the complete release of this dissolved O_2 species (after

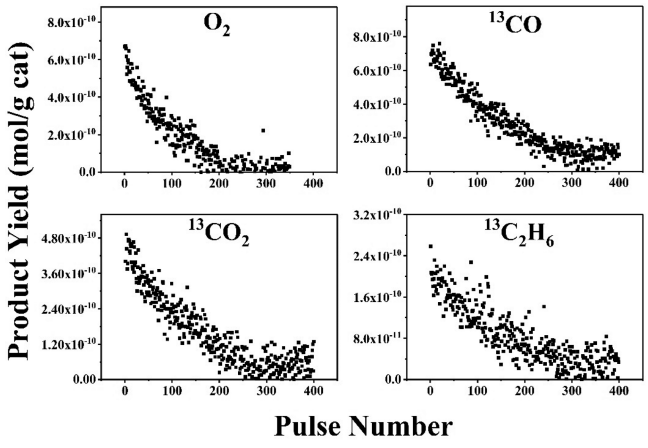

Figure 2. Yield of various products during anaerobic $^{13}CH_4$ series pulsing over $5Na_2WO_4/SiO_2$ catalyst at 800 °C. The corresponding $^{13}CH_4$ signal and conversion are shown in Figure S 3.

pulse number 150), generation of the OCM reaction products continued until up to ~350 pulses. This clearly indicates the presence of a second kind of oxygen species (that must be atomic in nature, lattice O) in the lattice of $5Na_2WO_4/SiO_2$ catalyst. The origin of lattice O species is assigned to the surface Na-WO_x phase since the only other oxide phase present in the catalyst is surface Na-WO_x sites. Additional support for this conclusion comes from anaerobic $^{13}CH_4$ series pulsing over the 0.5Na-$5WO_x/SiO_2$ catalyst, which registered both $^{13}CH_4$ conversion and production of ^{13}CO, $^{13}C_2H_6$ (see Figure S 4 and associated discussion). Further investigation shows that the amorphous bare SiO_2 and the crystalline cristobalite silica supports do not participate in the formation of dissolved O_2 and atomic lattice O species, confirming their origin from the molten Na_2WO_4 phase and surface Na-WO_x sites, respectively (see Figure S 5−S 7 and associated discussion).

■ PROMOTIONAL EFFECT OF MN

$^{16}O_2$-$^{18}O_2$ pump−probe experiments for 1.2Mn/SiO_2 and 1.2Mn-$5Na_2WO_4/SiO_2$ catalysts were performed to examine the promotional effect of Mn. The generation of $^{16}O_2$ and $^{16}O^{18}O$ products, induced by injection of the $^{18}O_2$ probe pulse, are shown in Figure S 11. Figure S 11a indicates that the total amount of $^{16}O_2$ released from 1.2Mn-$5Na_2WO_4/SiO_2$ catalyst is ~25% higher than the sum of $^{16}O_2$ released from $5Na_2WO_4/SiO_2$ and 1.2Mn/SiO_2 catalysts. To investigate this further, the height normalized pulse response of Ar and $^{16}O_2$ (after $^{18}O_2$ injection) are analyzed (see Figure 3). The identical Ar response curves for all catalysts indicate the uniformity of the experimental protocol (see Figure 3a). The $^{16}O_2$ desorption trends are strikingly different for all the catalysts. The $5Na_2WO_4/SiO_2$ catalyst exhibits the slowest $^{16}O_2$ desorption with a peak desorption time of 0.23 s (see Figure 3b). The 1.2Mn/SiO_2 catalyst shows the fastest $^{16}O_2$ desorption indicating MnO_x's ability to rapidly exchange oxygen between the gas-phase and the catalyst lattice (see Figure 3c). The addition of Mn to $5Na_2WO_4/SiO_2$ catalyst has multiple effects (see Figure 3d): (*i*) the desorption peak time of $^{16}O_2$ decreased, indicating that Mn addition improves the dissolved oxygen (O_2) exchange rate of $5Na_2WO_4/SiO_2$ catalyst and (*ii*) the $^{16}O_2$ desorption trend broadened significantly. The broadening effect in the low desorption time regime is

https://doi.org/10.1021/acscatal.1c02315
ACS Catal. 2021, 11, 10288−10293

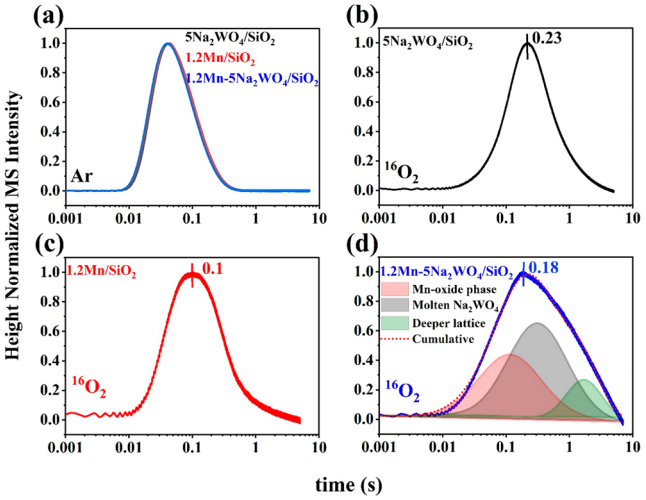

Figure 3. Height normalized mass-spectrometer response curves of Ar (a) and $^{16}O_2$ (b, c, and d) upon injection of $^{18}O_2$ in the $^{16}O_2$-$^{18}O_2$ pump−probe experiment (pump−probe spacing, Δt = 2 s) conducted over different catalysts at 800 °C. Plot (d) is deconvoluted into 3 parts to show the effect of Mn addition to $5Na_2WO_4/SiO_2$ catalyst. The cumulative trend of the three deconvoluted peaks is also shown by the dotted line in plot (d).

attributed to the release of oxygen species associated with the Mn-oxide phase (red highlighted area in Figure 3d). On the other hand, broadening in the high desorption time regime could be due to the release of additional dissolved oxygen species in the molten Na_2WO_4 phase that accounts for the excess 25% oxygen release (green highlighted area in Figure 3d).

The above observations indicate (*i*) the independent existence of the Mn-oxide phase and also (*ii*) the presence of interaction between Mn-oxide and molten Na_2WO_4 phases in 1.2Mn-$5Na_2WO_4/SiO_2$ catalyst. To further verify these phenomena, $^{13}CH_4$ series pulsing experiments were conducted for 1.2Mn/SiO_2 and 1.2Mn-$5Na_2WO_4/SiO_2$ catalysts (see Figure S 8 and Figure S 9 and associated discussion), and the selectivity values of the products were calculated (see Figure 4 and Figure S 10). From Figure 4, one can see that the $^{13}C_2H_6$ selectivity for $5Na_2WO_4/SiO_2$ catalyst remains constant between ∼25−30% over the range of $^{13}CH_4$ pulses (up to 100). For the 1.2Mn-$5Na_2WO_4/SiO_2$ catalyst, however, the $^{13}C_2H_6$ selectivity increases up to pulse number 30 and remains fairly constant at the higher pulse numbers. The discrepancy in the $^{13}C_2H_6$ selectivity values of $5Na_2WO_4/SiO_2$ and 1.2Mn-$5Na_2WO_4/SiO_2$ catalysts, in the first 30 pulses, can be attributed to the dominating contribution of Mn-oxide (present as a separate oxide phase) in 1.2Mn-$5Na_2WO_4/SiO_2$ catalyst (compare the $^{13}C_2H_6$ selectivity trend with 1.2Mn/SiO_2 catalyst in Figure 4). For a pulse number higher than 30, the $^{13}C_2H_6$ selectivity of $5Na_2WO_4/SiO_2$ and 1.2Mn-$5Na_2WO_4/SiO_2$ catalysts remains fairly constant. However, the significantly higher $^{13}C_2H_6$ selectivity (∼45−50%) observed for 1.2Mn-$5Na_2WO_4/SiO_2$ catalyst further confirms the promotion effect of Mn on molten Na_2WO_4 phase and surface Na-WO_x sites (through close interation between Mn-oxide, molten Na_2WO_4, and surface Na-WO_x phases).

Additional investigations regarding the effect of Mn toward oxygen dissociation (see Figure S 11 and Figure S 12 and associated discussion section) indicate that (*i*) when Mn is present alone (1.2Mn/SiO_2 catalyst), it is capable of

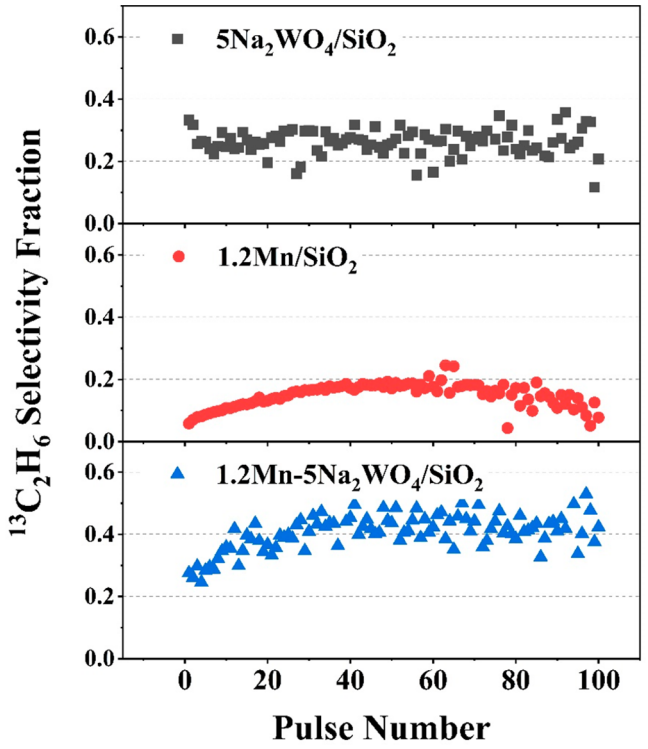

Figure 4. $^{13}C_2H_6$ selectivity fraction for various catalysts. The original data used for this are presented in Figure 2 ($5Na_2WO_4/SiO_2$ catalyst), Figure S 8 (1.2Mn/SiO_2 catalyst), and Figure S 9 (1.2Mn-$5Na_2WO_4/SiO_2$ catalyst).

dissociating molecular O_2 to form large amounts of $^{16}O^{18}O$ scrambled products, and (*ii*) addition of Mn to $5Na_2WO_4/SiO_2$ catalyst does not result in the increase of oxygen dissociation capability.

In conclusion, the supported $5Na_2WO_4/SiO_2$ catalyst possesses two distinct kinds of oxygen species at 800 °C: (*i*) a dissolved molecular O_2 type species only released from the molten Na_2WO_4 phase and (*ii*) an atomic lattice O type species associated with surface Na-WO_x sites that can be removed by reduction with CH_4. Both these oxygen species are catalytically active for the OCM reaction. Moreover, the 1.2Mn/SiO_2 catalyst also releases molecular O_2 type species associated with the Mn-oxide phase. However, these O_2 species associated with the Mn-oxide phase are highly unselective toward C_2 product formation. The addition of Mn to $5Na_2WO_4/SiO_2$ catalyst (*i*) accelerates the release of dissolved O_2 species, (*ii*) increases the total availability of dissolved O_2 species, (*iii*) improves the selectivity of dissolved O_2 and lattice atomic O species toward C_2 product formation, and (*iv*) does not improve gas-phase O_2 dissociation capability of 1.2Mn-$5Na_2WO_4/SiO_2$ catalyst. The above findings add clarity to the debate in the OCM literature regarding the active oxygen species present in the supported Mn-Na_2WO_4/SiO_2 catalyst, and future studies will contribute toward deciphering the complex OCM reaction mechanism.

■ ASSOCIATED CONTENT

Supporting Information

The Supporting Information is available free of charge at https://pubs.acs.org/doi/10.1021/acscatal.1c02315.

Experimental Details; Results and Discussion (Table S 1, Figures S 1−S 12) (PDF)

https://doi.org/10.1021/acscatal.1c02315
ACS Catal. 2021, 11, 10288−10293

Data Availability: The data sets generated during the current study are available from the corresponding authors upon reasonable request.

AUTHOR INFORMATION

Corresponding Authors

Yixiao Wang − *Biological and Chemical Science and Engineering, Energy Environment Science & Technology, Idaho National Laboratory, Idaho Falls, Idaho 83415, United States;* orcid.org/0000-0002-1446-3634; Email: yixiao.wang@inl.gov

Jonas Baltrusaitis − *Department of Chemical and Biomolecular Engineering, Lehigh University, Bethlehem, Pennsylvania 18015, United States;* orcid.org/0000-0001-5634-955X; Email: job314@lehigh.edu

Rebecca R. Fushimi − *Biological and Chemical Science and Engineering, Energy Environment Science & Technology, Idaho National Laboratory, Idaho Falls, Idaho 83415, United States;* orcid.org/0000-0002-7570-0234; Email: rebecca.fushimi@inl.gov

Israel E. Wachs − *Department of Chemical and Biomolecular Engineering, Lehigh University, Bethlehem, Pennsylvania 18015, United States;* orcid.org/0000-0001-5282-128X; Email: iew0@lehigh.edu

Authors

Sagar Sourav − *Biological and Chemical Science and Engineering, Energy Environment Science & Technology, Idaho National Laboratory, Idaho Falls, Idaho 83415, United States; Department of Chemical and Biomolecular Engineering, Lehigh University, Bethlehem, Pennsylvania 18015, United States;* orcid.org/0000-0001-5892-1329

Daniyal Kiani − *Department of Chemical and Biomolecular Engineering, Lehigh University, Bethlehem, Pennsylvania 18015, United States;* orcid.org/0000-0002-9748-3007

Complete contact information is available at: https://pubs.acs.org/10.1021/acscatal.1c02315

Notes

The authors declare no competing financial interest.

ACKNOWLEDGMENTS

S.S., Y.W., and R.R.F. gratefully acknowledge the support from the U.S. Department of Energy (USDOE), Office of Energy Efficiency and Renewable Energy (EERE), Advanced Manufacturing Office Next Generation R&D Projects under contract no. DE-AC07-05ID14517. D.K., J.B., and I.E.W. gratefully acknowledge the National Science Foundation (NSF) Chemical, Bioengineering, Environment and Transport Systems (CBET) award no. 1706581. S.S., D.K., J.B., and I.E.W. also sincerely thank Dr. Michael E. Ford of the *Operando* Molecular Spectroscopy & Catalysis Research Laboratory, Lehigh University, for his insightful input. S.S., Y.W., and R.R.F. thank James P. Pittman of Idaho National Laboratory for his help in the lab in preparing the isotope gas mixtures and conducting TAP experiments.

REFERENCES

(1) Wang, B.; Albarracín-Suazo, S.; Pagán-Torres, Y.; Nikolla, E. Advances in methane conversion processes. *Catal. Today* **2017**, *285*, 147−158.

(2) Arndt, S.; Otremba, T.; Simon, U.; Yildiz, M.; Schubert, H.; Schomäcker, R. Mn-Na_2WO_4/SiO_2 as catalyst for the oxidative coupling of methane. What is really known? *Appl. Catal., A* **2012**, *425*−*426*, 53−61.

(3) Kiani, D.; Sourav, S.; Baltrusaitis, J.; Wachs, I. E. Oxidative Coupling of Methane (OCM) by SiO_2-Supported Tungsten Oxide Catalysts Promoted with Mn and Na. *ACS Catal.* **2019**, *9*, 5912−5928.

(4) Beck, B.; Fleischer, V.; Arndt, S.; Hevia, M. G.; Urakawa, A.; Hugo, P.; Schomäcker, R. Oxidative coupling of methane—A complex surface/gas phase mechanism with strong impact on the reaction engineering. *Catal. Today* **2014**, *228*, 212−218.

(5) Fleischer, V.; Steuer, R.; Parishan, S.; Schomäcker, R. Investigation of the surface reaction network of the oxidative coupling of methane over $Na_2WO_4/Mn/SiO_2$ catalyst by temperature programmed and dynamic experiments. *J. Catal.* **2016**, *341*, 91−103.

(6) Gordienko, Y.; Usmanov, T.; Bychkov, V.; Lomonosov, V.; Fattakhova, Z.; Tulenin, Y.; Shashkin, D.; Sinev, M. Oxygen availability and catalytic performance of $NaWMn/SiO_2$ mixed oxide and its components in oxidative coupling of methane. *Catal. Today* **2016**, *278*, 127−134.

(7) Lomonosov, V. I.; Gordienko, Y. A.; Sinev, M. Y.; Rogov, V. A.; Sadykov, V. A. Thermochemical Properties of the Lattice Oxygen in W, Mn-Containing Mixed Oxide Catalysts for the Oxidative Coupling of Methane. *Russian Journal of Physical Chemistry A* **2018**, *92*, 430−437.

(8) Pak, S.; Qiu, P.; Lunsford, J. H. Elementary reactions in the oxidative coupling of methane over $Mn/Na_2WO_4/SiO_2$ and $Mn/Na_2WO_4/MgO$ catalysts. *J. Catal.* **1998**, *179*, 222−230.

(9) Aydin, Z.; Kondratenko, V. A.; Lund, H.; Bartling, S.; Kreyenschulte, C. R.; Linke, D.; Kondratenko, E. V. Revisiting Activity- and Selectivity-Enhancing Effects of Water in the Oxidative Coupling of Methane over MnO_x-Na_2WO_4/SiO_2 and Proving for Other Materials. *ACS Catal.* **2020**, *10*, 8751−8764.

(10) Werny, M. J.; Wang, Y.; Girgsdies, F.; Schlögl, R.; Trunschke, A. Fluctuating Storage of the Active Phase in a Mn-Na_2WO_4/SiO_2 Catalyst for the Oxidative Coupling of Methane. *Angew. Chem., Int. Ed.* **2020**, *59*, 14921−14926.

(11) Hou, S.; Cao, Y.; Xiong, W.; Liu, H.; Kou, Y. Site Requirements for the Oxidative Coupling of Methane on SiO_2-Supported Mn Catalysts. *Ind. Eng. Chem. Res.* **2006**, *45*, 7077−7083.

(12) Vamvakeros, A.; Jacques, S.; Middelkoop, V.; Di Michiel, M.; Egan, C.; Ismagilov, I.; Vaughan, G.; Gallucci, F.; van Sint Annaland, M.; Shearing, P.; et al. Real time chemical imaging of a working catalytic membrane reactor during oxidative coupling of methane. *Chem. Commun.* **2015**, *51*, 12752−12755.

(13) Yildiz, M.; Aksu, Y.; Simon, U.; Otremba, T.; Kailasam, K.; Göbel, C.; Girgsdies, F.; Görke, O.; Rosowski, F.; Thomas, A.; Schomäcker, R.; Arndt, S. Silica material variation for the Mn_xO_y-Na_2WO_4/SiO_2. *Appl. Catal., A* **2016**, *525*, 168−179.

(14) Matras, D.; Vamvakeros, A.; Jacques, S.; Grosjean, N.; Rollins, B.; Poulston, S.; Stenning, G. B. G.; Godini, H.; Drnec, J.; Cernik, R. J.; Beale, A. M. Effect of thermal treatment on the stability of Na-Mn-W/SiO_2 Catalyst for the Oxidative Coupling of Methane. *Faraday Discuss.* **2021**, *229*, 176−196.

(15) Vamvakeros, A.; Matras, D.; Jacques, S. D. M.; di Michiel, M.; Price, S. W. T.; Senecal, P.; Aran, M. A.; Middelkoop, V.; Stenning, G. B. G.; Mosselmans, J. F. W.; Ismagilov, I. Z.; Beale, A. M. Real-time multi-length scale chemical tomography of fixed bed reactors during the oxidative coupling of methane reaction. *J. Catal.* **2020**, *386*, 39−52.

(16) Kiani, D.; Sourav, S.; Wachs, I. E.; Baltrusaitis, J. Synthesis and molecular structure of model silica-supported tungsten oxide catalysts for oxidative coupling of methane (OCM). *Catal. Sci. Technol.* **2020**, *10*, 3334−3345.

(17) Kiani, D.; Sourav, S.; Taifan, W.; Calatayud, M.; Tielens, F.; Wachs, I. E.; Baltrusaitis, J. Existence and Properties of Isolated Catalytic Sites on the Surface of β-Cristobalite-Supported, Doped Tungsten Oxide Catalysts (WO_x/β-SiO_2, Na-WO_x/β-SiO_2, Mn-WO_x/β-SiO_2) for Oxidative Coupling of Methane (OCM): A Combined

Periodic DFT and Experimental Study. *ACS Catal.* **2020**, *10*, 4580−4592.
(18) Morgan, K.; Maguire, N.; Fushimi, R.; Gleaves, J. T.; Goguet, A.; Harold, M. P.; Kondratenko, E. V.; Menon, U.; Schuurman, Y.; Yablonsky, G. S. Forty years of temporal analysis of products. *Catal. Sci. Technol.* **2017**, *7*, 2416−2439.

https://doi.org/10.1021/acscatal.1c02315
ACS Catal. 2021, 11, 10288−10293